ISSN 0001-4338, Izvestiya, Atmospheric and Oceanic Physics, 2011, Vol. 47, No. 2, pp. 233–240. © Pleiades Publishing, Ltd., 2011.
Original Russian Text © V.G. Bondur, Yu.V. Grebenyuk, S.I. Muyakshin, K.D. Sabinin, 2011, published in Izvestiya AN. Fizika Atmosfery i Okeana, 2011, Vol. 47, No. 2, pp. 254–262.

Fine Vortex Columns on the Shelf in the Area of Bottom Convection Influence

V. G. Bondur[a], Yu. V. Grebenyuk[a], S. I. Muyakshin[b], and K. D. Sabinin[c]

[a] *Aerocosmos Scientific Center for Aerospace Monitoring, Gorokhovskii per. 4, Moscow, 105064 Russia*
e-mail: vgbondur@aerocosmos.info, grebenyk@gmail.com
[b] *Nizhni Novgorod State University, pr. Gagarina 23, Nizhni Novgorod, 603950 Russia*
e-mail: serg_mun@list.ru
[c] *Andreev Institute of Acoustics, Russian Academy of Sciences, ul. Shvernika 4, Moscow, 117036 Russia*
e-mail: ksabinin@yandex.ru

Received April 12, 2010

Abstract—This paper analyzes the results of investigations into extremely large releases of current velocities registered by an acoustic Doppler profiler during experiments performed on the Hawaii shelf. An integral analysis of the variability of current fields relies on the profile data of current velocities, temperature, and acoustic-scattering layers. Based on these investigations, we proposed a hypothesis stating that the small-scale variability of currents in profiler data is conditioned by the passage of fine vortices emerging in the outflow and rise of freshened waters from a subsurface sink near the shelf edge. To confirm this hypothesis on the emergence mechanism of the observed releases of current velocities, we conducted a mathematical simulation of the response that the Doppler meter has to the passage of fine vortex, which revealed a good agreement between model calculations and experimental data. Similar phenomena were also found in the Gelendzhik Bay of the Black Sea.

Keywords: Doppler profiler, velocity profile, soliton, isotherm, internal wave, isotherm, vortex column, bottom convection.

DOI: 10.1134/S0001433811020022

INTRODUCTION

Using measurement data on the characteristics of current velocities on the Hawaii shelf (the Mamala Bay) obtained with the help of an acoustic Doppler profiler, extremely large releases of current velocities were revealed. An integral analysis of the variability of current fields relies on the profile data of current velocities, temperature, and acoustic-scattering layers. Based on the results of these investigations, we proposed a hypothesis stating that the specific manifestations of the small-scale variability of currents in profiler data are related to fine vortices emerging in the outflow and rise of freshened waters from a subsurface sink near the shelf edge [1]. To confirm this hypothesis on the emergence mechanism of the releases of current velocities, we conducted a mathematical simulation of the response that the Doppler meter has to the passage of the fine vortex, which revealed a good agreement between model calculations and experimental data.

GENERAL CHARACTERISTICS OF MEASUREMENT METHODS AND RESULTING EXPERIMENTAL DATA

During a series of years in the basin of the Mamala Bay on the island of Oahu (Hawaii Islands), complex studies of anthropogenic influences on the ecosystem alongshore the basins caused by a subsurface sink have been performed to measure the characteristics of current velocities and temperatures using anchored thermal garlands and the bottom acoustic Doppler profilers (ADPs) of currents [2–7]. The allocation of stations where the vertical profiles of temperature (stations At, Bt, Ct) and three components of the vector of current velocities (stations Av, Bv, and Cv) were measured is shown in Fig. 1. The current velocities were measured at depths from 4 to 76 m with a step of 2 m in depth and 1 min in time. The measurements of water temperature were performed at different levels: from 3–18 to 45–76 m with a step between 30 s and 2–5 min.

An analysis of hydrophysical measurement data indicated that the Hawaii shelf (in the Mamala Bay) and other shelves are characterized by observed short-period internal waves conditioned by variations in the

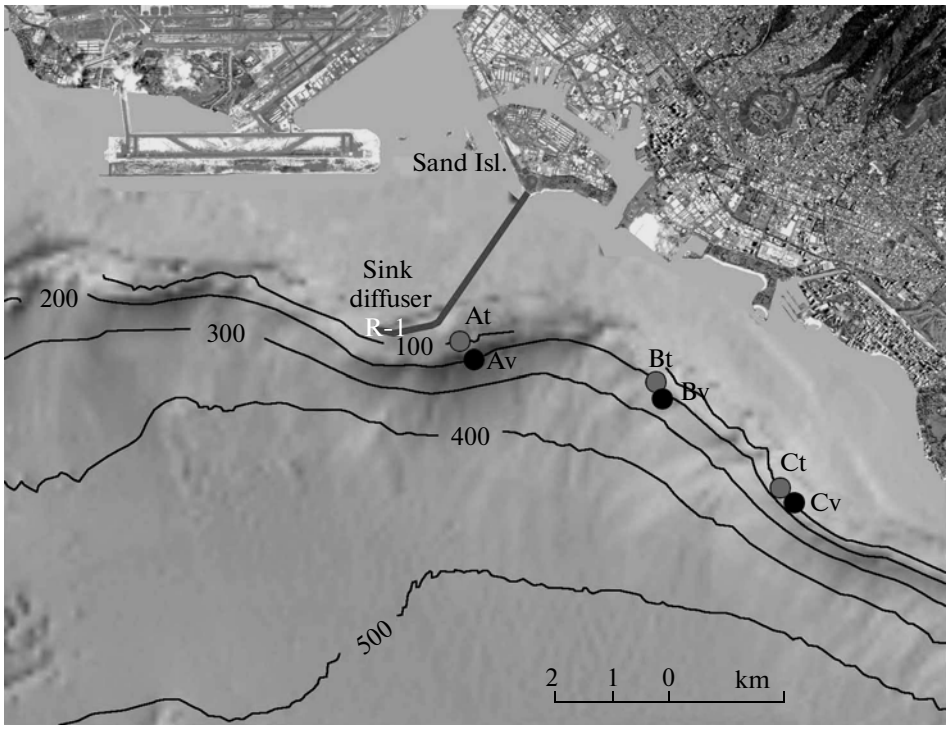

Fig. 1. Schematic of the allocation of stations for measuring temperatures and current velocities in Mamala Bay (Hawaii).

current fields and thermocline depths [2, 3, 6, 8, 9]. The time scales of these oscillations are usually several tens of minutes, although strong variations of environmental parameters in high-intensity solitons occur for a few minutes [8, 9]. At the same time, on the shelf of the Mamala Bay one can find even sharper variations reflected on bottom ADP records, when strong pulse bursts of horizontal currents are fixed with a sudden alternation of their direction up to the opposite over only a single minute. In this case there are usually variations in both the horizontal and vertical components of current velocities [1, 10].

INTEGRAL ANALYSIS OF THE RESULTS OF MEASUREMENTS OF CURRENT VELOCITIES, SCATTERING COEFFICIENTS, AND TEMPERATURE

An analysis of the characteristics of current velocities measured by the ADP in the Mamala Bay revealed large releases in their velocities with the probability of their manifestation being significantly higher than the values for the Gaussian process [1, 10]. Extreme releases of current velocities were observed at all stations during the measurement period from 2002 to 2004 both in original currents and in their high-frequency components (above 10 cycles/h).

An analysis of the measurement data indicated that the amplitude of releases of horizontal velocities reaches ±30 cm/s at an rms error of measurements of around 4 cm/s and their length is no more than 2 min [1, 10]. Both unipolar (positive or negative impulses) and bipolar releases (when the polarity of an impulse is changed through a step of 1 min) are observed. The bipolar impulse releases of current velocities are observed significantly more rarely than unipolar ones, although they are of greatest interest.

The observed bursts of current velocities could be related to the effect of proper motions of active scatterers, which is not ruled out in measurements with an acoustic profiler, or taken as measurement errors, but there are some peculiarities allowing one to doubt this overly simple explanation. First of all, in analyzing the impulses, care was taken to ensure that the field radiated by the ADP is free of fish shoals, which through their own motions might lead to bursts of velocity calculated on the basis of ADP data. Clusters of active scatterers are normally well manifested in the rate of scattering of the acoustic-profiler signals [11, 12]. It also seems improbable that erroneous bursts can emerge concurrently at many levels (see, for example, Fig. 2–4).

To reduce the errors, we smoothed the measurement data by depth using a low-frequency third-order Butterworth filter with a cutoff frequency of 100 cycles/km (smoothing each 10 m). Strong releases are observed both in original values of currents U, V, W and in their high-frequency components. One can judge the frequency of impulse bursts of current veloc-

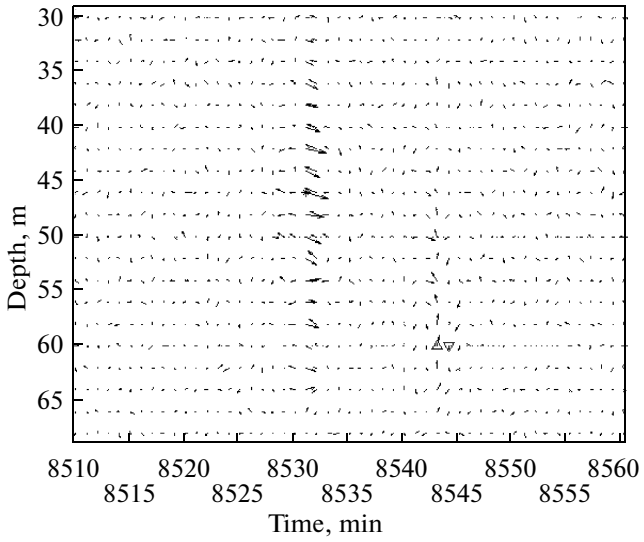

Fig. 2. Example of observed bipolar impulse bursts of high-frequency components of current velocities at station Av in 2003; the position of maximum of horizontal velocity (36 cm/s) is marked by an asterisk and the positions of extremums of vertical velocity (6 and –4 cm/s) are marked by triangles with vertices up and down, respectively; the velocity of the average current is 18 cm/s and the azimuth is 253°. The axis of the ordinate denotes the observation time in minutes at the given station.

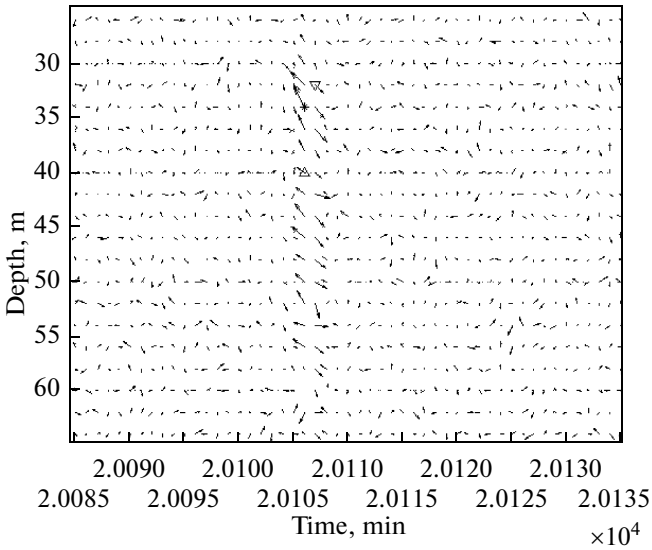

Fig. 3. Example of observed bipolar impulse bursts of high-frequency components of current velocities at station Bv in 2004; the position of velocity maximum (42 cm/s) at the 20106th min is marked by an asterisk and the positions of maximum (+6 cm/s) minimum (–5 cm/s) are marked by triangles with vertices up and down, respectively; the velocity of the average current is 14 cm/s and the azimuth is 120°. The axis of the ordinate denotes the observation time in minutes at the given station.

ities in given basins according the results of an analysis of current fields for a period of 19 days in 2004 at the station Bv (27370 samples with a step of 1 min at each level). At this station, at depths of 12 to 70 m, there were 920 impulses satisfying the condition that their amplitude exceeds the rms error of measurements no less than 3.5 times. In percentile values, the number of such releases at a single level is 0.11%, which significantly exceeds the figures of the Gaussian process (0.046%). The highest irregularities have the form of bipolar impulses. Examples of such impulses can be found in Figs. 2–4.

When explaining the reasons for strong releases of current velocities, we checked first whether they are caused by the passage of internal-wave solitons, which are accompanied with a shift in the isotherm depths. The current releases conditioned by solitons can be determined from the results of a combined analysis of current velocities, temperature, and acoustic-scattering layers [11–13]. To this end we conducted a thorough analysis of these characteristics for two types of sudden variability of the water medium: in solitons and bipolar impulse bursts of currents. In a thorough analysis of current fields, minutely profiles of their velocities, as well as temperature and rate of signal scattered by acoustic-scattering layers (ASLs), were used. The minutely profiles of currents were measured with the help of bottom ADPs installed near the shelf edge and the temperature oscillations were measured on garlands fixed (Fig. 1).

In the soliton registered at the station Bv in 2004 (see Fig. 5), the thermocline at the 13560th minute of observations (the measurements started at 10:59 on August 20, 2004) zoomed upward 18 m in only 3 min, which was also reflected in the field of acoustic-scattering layers, and the current velocity increased twofold (up to 15 cm/s) with a sharp turn toward the northeastern direction. The extremums of vertical velocities reaching +4 and –5 cm/s were observed on both sides of the maximum of the horizontal velocity, which is as it should be in solitons [13].

The sharpest releases of current velocities registered with the help of ADPs had the form of bipolar impulses when the amplification of currents was accompanied with their turn to the opposite direction in almost the whole layer of measurements. Examples of typical bipolar impulse bursts of current velocities registered at all observation points Av, Bv, and Cv are shown in Figs. 2–4. Let us consider in more detail the impulse bipolar burst of currents registered at the station Bv in 2004 at the 20106–20107th minute of measurements (see Fig. 3). Here, like in other cases of such bursts observed in all ADPs, weak chaotic high-frequency currents were suddenly replaced by currents that were sharply amplified and directed similarly in almost the whole water column. Here, the direction of currents suffers a stepwise change in the opposite direction as early as in the next minute. The 2004 measurement data contained 25 such impulse bursts. Interestingly, unlike solitons, the burst times of hori-

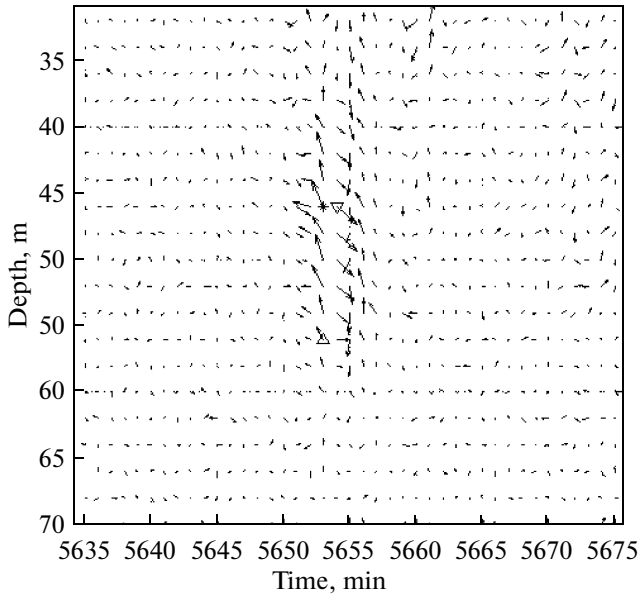

Fig. 4. Example of observed bipolar impulse bursts of high-frequency components of current velocities at station Cv in 2004; the position of velocity maximum (40 cm/s) at the 5654th min is marked by an asterisk and the positions of maximum (+5 cm/s) minimum (−4 cm/s) are marked by triangles with vertices up and down, respectively; the velocity of the average current is 15 cm/s and the azimuth is 310°. The axis of the ordinate denotes the observation time in minutes at the given station.

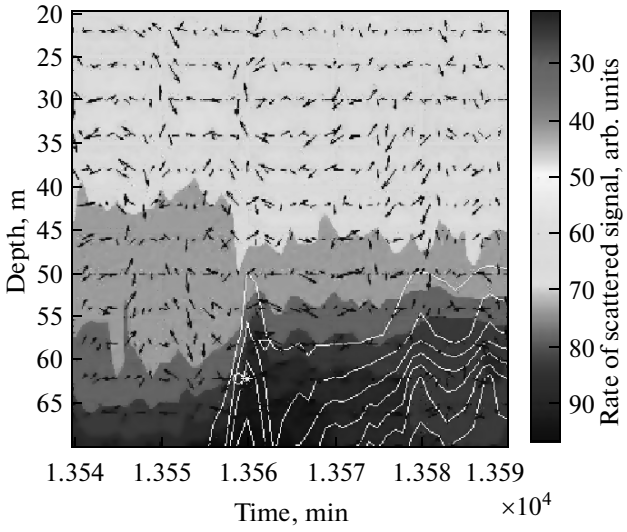

Fig. 5. Manifestation of a typical soliton in the Mamala Bay in the field of currents, temperature, and acoustic-scattering layers. The vectors of current velocities are demonstrated (arrows; north is up). The position of velocity maximum (15 cm/s) is marked by an asterisk and the positions of extremums of vertical velocity (+4 and −5 cm/s) are marked by a circle and a triangle, respectively. The isotherms (white lines) are constructed on the basis of data from a moored garland near ADP.

zontal velocities coincide with the times of extremums of the vertical velocity of currents (see Fig. 3).

A garland was installed to conduct temperature measurements at 8 levels in the range between 19 and 72 m (see Fig. 1) a small distance from the point of current-profile measurements (61 km east-southeastward with azimuth 111°). Figure 6 shows the plot of isotherm oscillations for the time period under consideration. It can be seen from this plot that, at the 20112th minute, a weak 1- to 3-m rise of isotherms occurred, which can be connected to the fact that an inhomogeneity passed over the garland, causing a sharp burst of current velocity in ADP (this occurred 6 min earlier). Under the action of the average current (velocity 0.14 m/s, azimuth 120°) existing in this area, the inhomogeneity transported by this current should have passed over the garland 7 min after the ADP passage. This almost coincides with the measured time shift of 6 min between the manifestation of inhomogeneity at the given points and corresponds to the transport rate of around 0.2 m/s. Based on the 1-m rise of isotherms in a minute between the levels of 59 and 63 m, where the thermistors were closest (and, consequently, the vertical shift could be estimated most accurately), we found that the vertical velocity of the current is around 1 cm/s, which is considerably smaller than the value measured by the ADP (+9 and −5 cm/s).

MODELING THE ADP RESPONSE ON VORTEX STRUCTURE PASSAGE

To explain the observed releases, we proposed a hypothesis stating that the specific manifestations of the small-scale variability of currents in ADP data obtained on the shelf in the area of subsurface sink influence are most likely related to fine vortices (vortex columns) emerging in the outflow and rise of freshened waters from the diffuser [1, 10]. To confirm this hypothesis, it is necessary to find how the passage of such a fine vortex through ADP rays will be reflected in ADP indications.

An acoustic Doppler current profiler (ADCP; in this paper, the abbreviation ADP is used) is a 3- or 4-beam impulse hydrolocator [14]. Its rays are located symmetrically relative to the vertical axis and are deviated from it at similar angles. An echo signal taken by each ray is analyzed in adjacent time windows to yield a Doppler frequency shift Δf, which is proportional to the projection of the rate of scatterers relative to an antenna on the ray axis V_r:

$$\Delta f = 2f_0 V_r / C_s,$$

where f_0 is the carrier frequency and C_s is the sound speed.

Knowing the delay of certain window t_w, one can localize the position of the corresponding element of distance (ED) relative to the antenna: $r = C_s t_w/2$.

The algorithm of ADP data processing is based on the assumption that the current velocity is constant for all EDs located at a certain depth. With the help of ADP, the velocities are measured correctly only if the scale of current inhomogeneities is considerably larger than the distance between the ADP rays [14]. Minute shifts of velocity in the ADP indications cannot be caused by sufficiently large spatial scales and therefore testify only about inhomogeneity of the current field between ADP rays. Because of this, strictly speaking, with the help of ADP, one cannot obtain the correct pattern of currents in a fine inhomogeneity like the vortex column (a vortex whose height is considerably higher than its diameter).

To confirm the hypothesis that the impulse bursts of currents are conditioned by the passage of fine vortices through ADP rays, we conducted a mathematical simulation of its response on the nearby passage of a vertical vortex with a spatial scale that is considerably smaller than the distance between it rays (and EDs). By ADP response we mean the time realizations of three values that, in the case of a homogeneous field of current velocity, would be its projections V_X, V_Y, V_Z on the axis of the Cartesian coordinate system related to the instrument. It is reasonable to direct the vertical axis Z of this "instrument" coordinate system along the symmetry axis of its antenna system. Then, for a three-ray version of the instrument, which was applied in our case, these projections can be calculated with the help of the following matrix transformation

$$\begin{pmatrix} \frac{-2}{3\sin\Theta} & \frac{1}{3\sin\Theta} & \frac{1}{3\sin\Theta} \\ 0 & \frac{-1}{\sqrt{3}\sin\Theta} & \frac{1}{\sqrt{3}\sin\Theta} \\ \frac{1}{3\cos\Theta} & \frac{1}{3\cos\Theta} & \frac{1}{3\cos\Theta} \end{pmatrix} \begin{pmatrix} V1 \\ V2 \\ V3 \end{pmatrix} = \begin{pmatrix} Vx \\ Vy \\ Vz \end{pmatrix}. \quad (1)$$

Here, V_i, $i = 1, 2, 3$, are the projections of current velocity on ADP-ray axes and Θ is the angle of deviation of ray axes from the vertical ($\Theta = 25°$).

To model the time dependence of output variables of the instrument, it is necessary to calculate the changes of these projections for different vortex positions relative to ADP. As a model, we take the so-called "Rankin vortex," which is a cylindrical vortex with a vertical axis and solid-body rotation into the internal domain with a radius of R_0, where the velocity grows linearly with the growing distance from the center up to the maximum value V_{max}, and then it declines back proportional to the distance in line with the law $V = V(R_0)R_0/R$. Thus, we do not consider vertical velocities (see above) and take the current to be the vortex current in the internal domain and potential current in the external domain. Let us set the values $R_0 = 5$ m and $V_{max} = 0.5$ m/s corresponding to the estimates of vortex parameters described in [1].

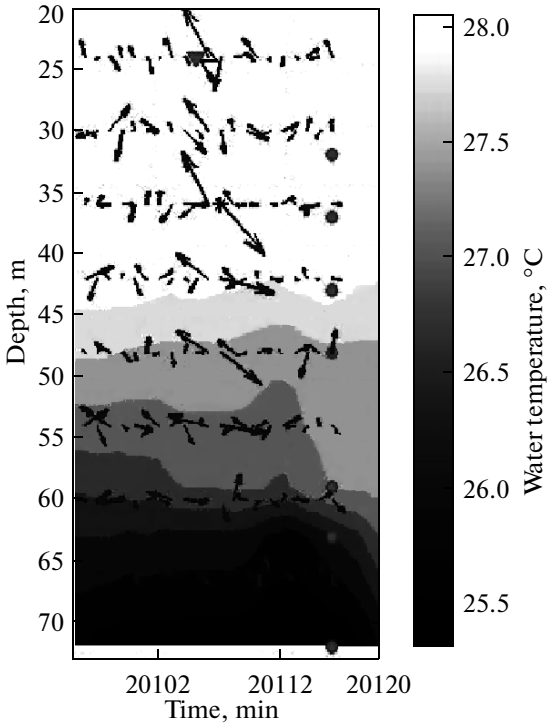

Fig. 6. Oscillations of isotherms (shades) and vector of high-frequency currents (arrows) near the impulse burst of currents shown in Fig. 4. From the side, circles denote the location of temperature sensors according to depth.

Strictly speaking, a simulation of the vortex passage should involve the velocity of the homogeneous motion transporting it. However, as was noted above, the experimental realizations of velocity were subjected to high-frequency filtering before analysis. Therefore, the rate of transport was not considered and only deviations from it were taken into account. To simulate the ADP response on the vortex passage, we developed a scheme for calculating the projections of liquid velocity on the instrument rays V_i depending on the distance between the vortex and the instrument center and EDs.

Because the current field is of cylindrical symmetry relative to the vortex axis, when simulating the ADP response to the vortex passage it turned out to be convenient to consider the instrument transport relative to the vortex rather than the instrument. The position of the instrument center (the point with the outgoing projections of its rays on the horizontal plane) is specified relative to the vortex axis by coordinates X and Y. The length of ray projections is denoted by D. This value depends on the height over the bottom Z_0 of the layer where the velocity is measured:

$$D = \tan(\Theta)Z_0.$$

r_0 is the distance from the vortex center to the instrument center and r_i ($i = 1, 2, 3$) are the distances from the vortex center to corresponding EDs. Then,

the projections of current velocity on rays can be expressed as

$$V_i = V(r_i)\sin\left(\arccos\left(\frac{D^2 + (r_i^2 - r_0^2)}{2Dr_i}\right)\right)\sin(\Theta). \quad (2)$$

In this formula, we have $i = 1, 2, 3$, and

$$r_0 = \sqrt{X^2 + Y^2}, \quad (3)$$

$$r_1 = \sqrt{X^2 + (D + Y)^2}, \quad (4)$$

$$r_2 = \sqrt{\left(X - D\sin(\pi/3)\right)^2 + \left(Y - D\cos(\pi/3)\right)^2}, \quad (5)$$

$$r_3 = \sqrt{\left(X + D\sin(\pi/3)\right)^2 + \left(Y - D\cos(\pi/3)\right)^2}, \quad (6)$$

$$V(r) = \begin{cases} V_{\max}\dfrac{r}{R_0} & \text{for} \quad r \le R_0, \\ V_{\max}\dfrac{R_0}{r} & \text{for} \quad r \ge R_0. \end{cases} \quad (7)$$

For calculations with the help of formulas (1)–(7), we developed a MATLAB program. For validation purposes, we computed the instrument response on the "big" vortex passing exactly through its center along the *OX*-axis. In other words, it was assumed that $D \ll R_0$. It is apparent that the condition of local homogeneity of current velocity is satisfied in the vortex for almost the whole field of the current. This condition is violated only at the boundary $R = R_0$. In this case, a spurious release of the vertical velocity component occurs, which vanishes away from the boundary with high accuracy. Similar releases are also observed in experimental data. The behavior of the component V_Y is consistent with the model field, and V_X also demonstrates spurious releases at the boundary of the "solid-body" part of the vortex.

Using this program, we simulated the instrument response to the vortex passing over it.

The ADP response on the vortex passage depends on many parameters, including, first and foremost, the direction of the vortex rotation, the velocity and direction of its movement, the position of the vortex trajectory relative to the ADP, the orientation of vortex rays, the measurement resolution, and even the specific moments when the vortex passes over ADP while measurements were conducted (if the frequency of measurements is insufficient, a fine vortex cannot be reflected in measurements with sufficient details).

We performed calculations of current velocities for a wide range of vortex parameters and obtain the following results. The passage of fine vortices through ADP rays leads to the emergence of sharp releases in current velocities measured by the instrument. The amplitude of releases and their form (unipolar or bipolar) depend on the vortex allocation relative to the ADP and the direction of its movement.

Figures 7a and 7b show a comparison of model calculations (Fig. 7b) with data from field measurements (Fig. 7a) for current velocities conducted at station Bv in 2004 at the 20095–20115th min. Among the many variants considered, the pattern observed at this point is most resembled by the case when the anticyclonic vortex with the abovementioned parameters moves east-southeastward and its center is 20 m away from (south-southwestward of) the ADP center (see the schematic in Fig. 7c). In other cases of model vortex passage relative to the instrument, the ADP response could be substantially changed, taking the form of a single burst and a less significant turn of the vector in the double impulse. In most cases this turn occurred in 1–2 min.

An analysis of Figs. 7a and 7b shows a good resemblance of model calculations with field measurement data. The close resemblance between the extremums of vertical velocities, not only in depth (33–40 m in Fig. 7a and 38 m in Fig. 7b) but also in magnitude (+6, –5 cm/s in Fig. 7a and ±6 cm/s in Fig. 7b), is particularly remarkable.

The vortex model used has no vertical motions at all; therefore, the presence of vertical velocities in the ADP response (see Fig. 7b) is an artifact related to the peculiarities of the response of this instrument. The coincidence of burst times of vertical and horizontal velocities in measurement data and calculation results is explained by the fact that the registered vertical velocities in this case are inconsistent with true motions and emerge due to the projection of horizontal currents in the vortex on inclined rays of ADP.

The temporal coincidence of bursts of vertical and horizontal velocities, which is characteristic for almost all registered impulses, is, as was already noted above, a characteristic differing them from internal waves, where the vertical and horizontal velocities are in the quadrature.

Let us consider in more detail the relationship between revealed bursts of current velocities and the rate of back acoustic scattering, but now from the point of view of admixture capture by vortices (as was observed, for example, in [15]), rather than in terms of the rare impact of active motions of scatterers on ADP indications.

Figures 8a–8c show the scattering rate from measurement data for station Bv in 2004 separately for three cases. An analysis of Figs. 8a–8c shows that the admixture concentration on the first ray was significantly weaker than on the second and third rays. This is consistent with the supposed vortex motion, the main part of which occurs first through the third ray and then through the second ray (see Fig. 7c). The scattering burst was best expressed on the third ray, where it coincided with the northwest maximum of velocity (the front end of vortex?). On the second ray it was less compact, and it manifests itself weakly on the first ray.

In general, the set of facts under consideration here can be explained well within the frameworks of the vortex hypothesis formulated in [1] and confirmed by

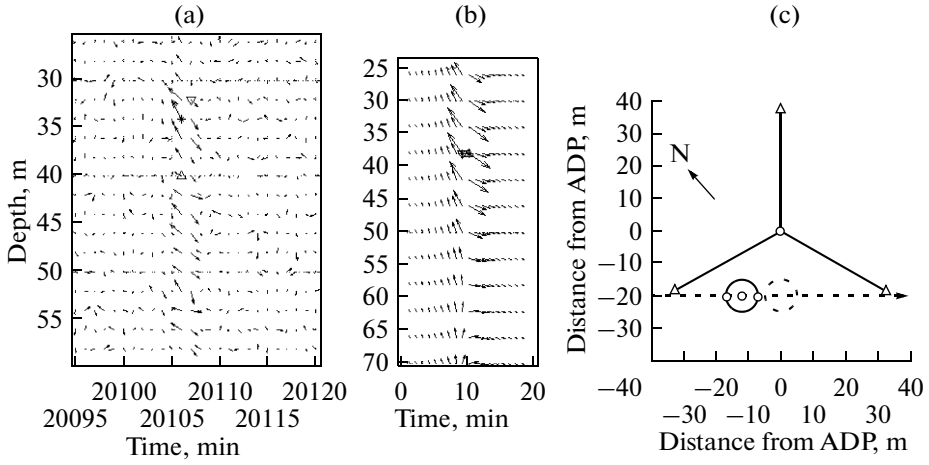

Fig. 7. (a) Impulse burst of high-frequency (above 10 cycles/h) currents registered at the 20106th min of measurements at station Bv in 2004. The vectors of sections (arrows; north is up). The position of velocity maximum (42 cm/s) is marked by an asterisk and the positions of extremums of vertical velocity (6 and −5 cm/s) are marked by triangles with vertices up and down, respectively. (b) Vector of currents by the model of ADP response to the anticyclonic Rankin vortex with parameters $R = 5$ m and $V_{max} = 0.5$ m/s, passing nearby the ADP southeastward with a velocity of 0.2 m/s (the vortex center is 20 m from (southwestward of) the ADP. The maximum of horizontal velocity reaches 29 cm/s and the extremums of vertical velocity are equal to ±6 cm/s. (c) Schematic of vortex motion; the three line segments exiting from a common point indicate the projections of ADP rays on the sea surface; the boundary of the central part of vortex where the orbital velocity reaches a maximum is shown by circles for the 9th (solid line) and 10th (dotted line) minutes of calculations, which corresponds to the 20106th and 20107th minutes of measurements; the arrow denotes the northward direction and the dotted line denotes the vortex trajectory.

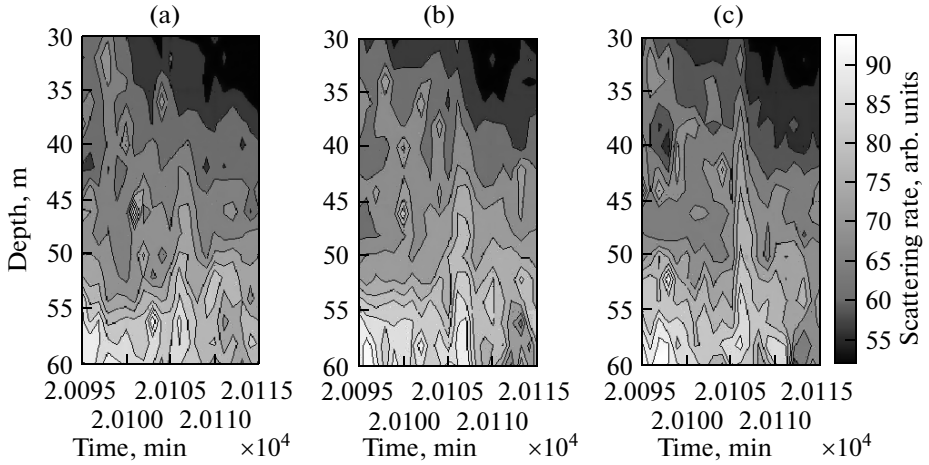

Fig. 8. Rate of scattered signal at different rays of station Bv in 2004 at the 20095–20110th minutes of observations: (a) ray 1 (northeastern); (b) ray 2 (southeastern); and (c) ray 3 (southwestern).

the results of a simulation of the ADP response to the passage of fine vortices.

We cannot also rule out the possibilities for other interpretations of resulting data; however, in our opinion, it is doubtful that the ocean has small-scale current inhomogeneities with amplitudes as large as in the impulse bursts described above. Even such a sharp phenomenon as solitons has much greater spatial scales and other relations between horizontal and vertical currents.

CONCLUSIONS

Based on the results of a thorough analysis, we investigated the characteristics of extremely large releases of current velocities registered by an acoustic Doppler profiler in the Mamala Bay and the possible reasons for their emergence. We proposed a hypothesis stating that the specific manifestations of the small-scale variability of currents are conditioned by fine vortices that can emerge on the shelf under the action of Doppler convection. Numerical simulations to the

response of the Doppler profiler of currents on the passage of fine vortex structures confirm the validity of this hypothesis.

In conclusion, we note that the emergence of vortex structures in the Mamala Bay is quite possible, if not inevitable: due to the subsurface sink of fresh waters of Honolulu, a strong convection over the shelf appears, the field of which can include small vortices like small dust vortices in the near-surface air observed in the warmest days over heated segments of the ground.

Some similarity to this vortex formation can be seen also in the results of laboratory experiments on convection in a rotating water volume, when a drop (sunk in water) of a heavier liquid generates a vortex concentrating the whole admixture in itself [15]. This concentration of admixture in vortices can also explain the increased rate of scattering within the many of impulse bursts that we observed.

It is important to note that, if the hypothesis on vortices in the convective layer is confirmed during the further field and laboratory experiments planned by the authors, some corrections should be made in our understanding of the pure diffusion transport of admixtures in the zone of influence of deep sinks, taking into account the admixture capture and transport of more or less long-living vortices. Let us also note that these phenomena can also emerge in other areas of the bottom unload of fresh ground waters entering the shelf from water-carrying layers from the coast, such as, for example, with the Crimean and Caucasian coasts, as well as in areas where gas torches emerge [16].

Measurements of current velocities in the basin of the Gelendzhik Bay with the help of bottom ADP near the deepwater sink of fresh waters also indicated that there are strong releases of currents like the ones considered above. The results of high-frequency components of velocity in Gelendzhik Bay will be published as a new paper.

REFERENCES

1. V. G. Bondur, Yu. V. Grebenyuk, and K. D. Sabinin, "Peculiar Discontinuities in Small Scale Flows at the Shelf in the Area of Natural Convection Impact," Dokl. Akad. Nauk **429** (1), 110–114 (2009).
2. V. G. Bondur, "Aerospace Methods in Modern Oceanology," in *New Ideas in Oceanology*, Vol. 1: *Physics. Chemistry. Biology* (Nauka, Moscow, 2004), pp. 55–117 [in Russian].
3. V. G. Bondur, "Complex Satellite Monitoring of Coastal Water Areas," in *Proc. of 31st Int. Symp. on Remote Sensing of Environment*, St. Petersburg, 2005, www.isprs.org., p. 7.
4. V. Bondur, R. Keeler, and C. Gibson, "Optical Satellite Imagery Detection of Internal Wave Effects from a Submerged Turbulent Outfall in the Stratified Ocean," Geophys. Res. Lett. **32**, L12610, doi: 10.1029/2005GL022390 (2005).
5. V. Bondur, R. Keeler, and D. Vithanage, "Sea Truth Measurements for Remote Sensing of Littoral Water," Sea Technol. **45**, 53–58 (2004).
6. V. G. Bondur, N. N. Filatov, Yu. V. Grebenyuk, et al., "Studies of Hydrophysical Processes during Monitoring of the Anthropogenic Impact on Coastal Basins Using the Example of Mamala Bay of Oahu Island in Hawaii," Okeanologiya **47** (6), 827–846 (2007) [Oceanology **47** (6), 769–787 (2007)].
7. V. G. Bondur, R. N. Keeler, S. A. Starchenkov, et al., "Monitoring of Pollution of the Coastal Water Areas of the Ocean using Multispectral Satellite Images of High Spatial Resolution," Issled. Zemli iz Kosmosa, No. 6, 42–49 (2006).
8. V. G. Bondur, Yu. V. Grebenyuk, and K. D. Sabinin, "Variability of Internal Tides in the Coastal Water Area of Oahu Island (Hawaii)," Okeanologiya **48** (5), 661–671 (2008) [Oceanology **48** (5), 611–621 (2008)].
9. V. G. Bondur, Yu. V. Grebenyuk, and K. D. Sabinin, "The Spectral Characteristics and Kinematics of Short-Period Internal Waves on the Hawaiian Shelf," Izv. RAN. Fizika Atmosfery i Okeana **45** (5), 641–651 (2009) [Izv., Atmos. Ocean. Phys. **45** (5), 598–607 (2009)].
10. V. Bondur, Yu. Grebenuk, and K. Sabinin, "Thin Vortexes in the Current Field of Mamala Bight (Hawaii)," in *Proc. of Int. Conf. Fluxes and Structures in Fluids*, (IPMech, Moscow, 2009), pp. 23–24.
11. I. B. Andreeva, "Sound Scattering Layers—Acoustic Inhomogeneity Thickness of Ocean Waters," Akust. Zh. **45** (4), 437–444 (1999).
12. Yu. G. Chindonova and V. A. Shulepov, "Sound Scattering Layers as Indicators of Internal Waves in the Ocean," Okeanologiya **5** (6), 550–554 (1965).
13. K. V. Konyaev and K. D. Sabinin, *Waves within the Ocean* (GIMIZ, St. Petersburg, 1992) [in Russian].
14. *Acoustic Doppler Profiler*, Software Manual, Ver. 6.42, (2000), pp. 1–30.
15. E. V. Stepanova and Yu. D. Chashechkin, "Anisotropic Impurity Transport in a Composite Vortex," Dokl. Akad. Nauk **423** (4), 474–478 (2008).
16. O. A. Karimova and I. S. Zektser, "Water under Water," Priroda (Moscow, Russ. Fed.), No. 9, 28–32 (2007).